

Bloch Oscillations of an Acoustic Field in a Layered Structure

A. A. Karabutov, Jr.^{a, b}, Yu. A. Kosevich^c, and O. A. Sapozhnikov^b

^a Institute on Laser and Information Technologies, Russian Academy of Sciences,
ul. Svyatoozerskaya 1, Shatura, Moscow oblast, 140700 Russia

e-mail: akarabutov@gmail.com

^b Moscow State University, Physics Faculty, Department of Acoustics, Moscow, 119991 Russia

e-mail: oleg@acs366.phys.msu.ru

^c Semenov Institute of Chemical Physics, Russian Academy of Sciences, ul. Kosygina 4, Moscow, 119991 Russia

e-mail: yukosevich@gmail.com

Received August 29, 2012

Abstract—This study is devoted to experimentally achieving the phenomenon of periodic modulation of the acoustic-wave intensity, which is observed upon passage of an acoustic signal through a quasi-periodic structure and is the acoustic analog of the effect of Bloch oscillations (BO). Ultrasound at a frequency of 1 MHz is used, and a layered structure that consists of alternate plane-parallel glass and water layers serves as a superlattice. In order to create an analog of the external electric field, the thickness of the water layers was changed inversely with respect to their ordinals. It is shown that the transmission spectrum of such a structure has the form of narrow equidistant peaks (an analog of the Wannier–Stark ladder), and the envelope of a transmitted signal undergoes periodic oscillations (analogous to BO). The experimental results are in good agreement with theoretical calculations performed by the transfer-matrix method.

Keywords: Bloch oscillations, Wannier–Stark ladder, quasi-periodic structures

DOI: 10.1134/S1063771013020061

INTRODUCTION

The Bloch oscillation (BO) effect characterizes the behavior of electrons in a solid to which an external electric field is applied [1, 2]. The BO effect is most simply described using the quasi-classical model. According to this model, when a stationary field is switched on, the electron quasi-momentum begins to increase as a linear function of time. Due to the periodicity of the structure in a solid, there is also spatial periodicity in the dependence of the electron energy on the quasi-momentum. Because the particle velocity in a quasi-classical description is equal to the derivative of the energy with respect to the quasi-momentum, the electron velocity is a periodic function of time for the linearly increasing quasi-momentum. In other words, oscillatory motion of electrons is initiated, and, therefore, an alternating current is generated in the solid. The frequency of such (Bloch) oscillations is $f_B = eEa/h$, where e is the electron charge, E is the electric field strength, a is the lattice spacing, and h is the Planck constant. This effect of current oscillations under the action of a stationary electric field contradicts the usual classical conceptions.

An alternative method for explaining BO is based on consideration of the electron energy levels. Stark splitting of the initially uniform electron energy spectrum into a set of equidistant lines, which are called

Wannier–Stark ladder, occurs upon application of a stationary external field [3]. The energy gap between these lines is $\Delta W = eEa$. Bloch oscillations occur at the frequency $f_B = \Delta W/h$ and represent quantum beats between states of the aforementioned Stark ladder [4].

In order to achieve BO, an electron must have enough time to change the direction of its motion before it undergoes scattering; thus, the following condition must be fulfilled: $eEl > W$, where l is the electron free path and W is the width of the permitted band. Therefore, in traditional semiconductors whose permitted bandwidths are several electronvolts, the observation of BO requires virtually unattainable electric fields of ~ 1 MV/cm. The possibility of avoiding this difficulty has appeared only recently owing to the development of technologies for growing solid-state heterostructures—superlattices [5]. The constant a of such nanostructured lattices exceeds the interatomic spacing by several tens of times, thus providing the condition for the appearance of BO in relatively moderate electric fields (1–10 kV/cm). The first indications of the BO effect were described in papers on superlattices based on GaAs/Al_xGa_{1-x}As semiconductor compounds [5–7]. The possible application of the BO effect is associated with the development on its basis of a special class of generators and receivers of electromagnetic waves at terahertz frequencies.

The BO effect related to the behavior of the electron wavefunction has analogs for waves of different natures (e.g., acoustic, optical, or spin waves) that propagate in appropriate quasi-periodic structures (QPSs) [8]. It is known that, along with semiconductor superlattices, another class of heterostructures exists (photon crystals). The refractive index of light periodically changes in such crystals; owing to this effect, permitted and forbidden bands appear (light-transmission and light-blocking). An experiment that involved observations of an optical BO analog was performed in [9]. Optical superlattices that were formed from layers with different refractive indices of light were investigated, which were grown in a certain succession. In order to create an analog of the Wannier–Stark ladder in the transmission spectrum, the authors of [9] changed the period of the heterostructure in inverse proportion to the layer number. In this case, the resonance frequencies of layers were proportional to the layer number, thus making the transmission spectrum of this structure equidistant. The produced structure was illuminated with a short light pulse, and the time dependence of the transmitted signal intensity was studied. As was predicted by calculations, after passing through the created structure, the signal had the form of a train of pulses with decaying amplitudes that followed one after another at a constant repetition rate.

The successful observation of the optical analog of BO initiated studies on the development of systems for observing BO for acoustic waves [10–13]. In these studies, waves also propagated in QPSs, and elements of such structures were chosen based on the condition that their resonance frequencies were proportional to their ordinal number. Different types of QPSs were used. For example, a one-dimensional medium in the form of a set of jointed elastic rods with circular or rectangular cross sections was used in [10]. Rods differed either in length (in the case of elements in the form of circular cylinders) or in height (in the case of elements in the form of parallelepipeds). Paper [11] described experiments in which a layered medium manufactured analogously to a photon crystal from [9] was used. The medium consisted of a set of alternate solid and fluid layers, into which aperiodicity was introduced by changing the thicknesses of fluid layers. The equidistant spectrum of sound transmission through a layered structure (an analog of the Wannier–Stark ladder) was measured in [11], but the transmitted-signal envelope oscillations themselves, which simulated BO, were not recorded. One of the objectives of this study was to perform such observations. This work is also devoted to studies of some features in the propagation of acoustic waves in layered media with a constant gradient of the reciprocal layer thickness.

THEORETICAL MODEL

Let us consider a layered medium that is a set of alternate layers of two different materials. For convenience of practical implementation of layers with a controlled thickness, we consider that one material is fluid and the other is solid. However, it should be noted that a particular type of layer material is of no significance for the theoretical simulation. Let the thickness of the solid layers be the same; the thickness of the fluid layers changes according to the law (see [9, 11])

$$l_m = \frac{l_0}{1 + \gamma(m - m_0)}, \quad (1)$$

where $m = 1, 2, \dots, M$ is the layer number, l_m is its thickness, $m_0 = M/2$ and l_0 are the layer number and layer thickness at the middle of the studied structure, respectively, and $\gamma = 1/l_{m+1} - 1/l_m$ is the relative gradient of the reciprocal thicknesses, which is assumed to be independent of layer number m .

A convenient method for analyzing the propagation of a harmonic wave in a medium that consists of uniform layers is the transfer-matrix method [14]. Recall the essence of this approach. Let $n = 1, 2, \dots, N$ be the layer number (e.g., $n = 1, 3, 5, \dots$ correspond to solid-state layers, and $n = 2m = 2, 4, 6, \dots$, to fluid layers); P_n^+ and P_n^- are the complex amplitudes of the acoustic pressure for waves that propagate in a given layer to the right and to the left. The following relationship can then be written for the amplitudes of waves in two neighboring layers [15]:

$$\begin{pmatrix} P_{n-1}^+ \\ P_{n-1}^- \end{pmatrix} = \hat{A}_{n-1,n} \begin{pmatrix} P_n^+ \\ P_n^- \end{pmatrix}. \quad (2)$$

Here, $\hat{A}_{n-1,n}$ is the transfer matrix:

$$\hat{A}_{n-1,n} = \begin{pmatrix} \frac{z_n + z_{n-1}}{2z_n} e^{-ik_n l_n} & \frac{z_n - z_{n-1}}{2z_n} e^{ik_n l_n} \\ \frac{z_n - z_{n-1}}{2z_n} e^{-ik_n l_n} & \frac{z_n + z_{n-1}}{2z_n} e^{ik_n l_n} \end{pmatrix}. \quad (3)$$

The elements $\hat{A}_{n-1,n}$ of the matrix depend on the acoustic impedances z_n , velocities of sound c_n , and layer thicknesses l_n . The following notation is used in (3): $k_n = \omega/c_n$ is the wavenumber and ω is the cyclic frequency. It is assumed that the character of the time dependence in a wave has the form $\sim e^{-i\omega t}$. When formulas of type (2) are written for all layers, we find that the incident and reflected waves in water (P_0^+ and P_0^-) are related via the matrix relationship to the incident and reflected waves behind all plates (P_N^+ and P_N^-):

$$\begin{pmatrix} P_0^+ \\ P_0^- \end{pmatrix} = \begin{pmatrix} a_{11} & a_{12} \\ a_{21} & a_{22} \end{pmatrix} \begin{pmatrix} P_N^+ \\ P_N^- \end{pmatrix}, \quad (4)$$

where the full transfer matrix $\hat{A} = \|\|a_{ij}\|$ is found by consecutive multiplication of the transfer matrices of all layers: $\hat{A} = \hat{A}_{0,1} \times \hat{A}_{1,2} \times \dots \times \hat{A}_{N-2,N-1} \times \hat{A}_{N-1,N}$.

We are interested in the situation where a plane-parallel structure of solid plates is immersed in the fluid, and the source of the incident wave and the receiver are to the left and right of the structure, respectively. It can then be considered that no counter-propagating wave is present in the last (fluid) layer: $P_N^- = 0$; the reflection coefficient and the coefficient of transmission through the structure can be expressed through (4): $R = P_0^-/P_0^+ = a_{21}/a_{11}$ and $T = P_N^+/P_0^+ = 1/a_{11}$. In order to calculate the values of the wave amplitudes in layers at the specified amplitude of the incident wave P_0^+ , algorithm (2) must be consecutively applied proceeding from values of $P_N^- = 0$ and $P_N^+ = TP_0^+$. When calculating the acoustic energy density in layers, it is also necessary to know the values of the vibrational velocity amplitudes: $V_n^\pm = \pm P_n^\pm/z_n$.

In order to recall the known features of the transmission spectrum of the layered structure, let us analyze the case of a homogeneous structure ($\gamma = 0$) at different parameters of the media that constitute this structure. This consideration can be simplified by using a matrix that describes the propagation of acous-

tic waves through two layers at once. The sought matrix can be obtained as a result of the product of matrices (3) for solid and fluid layers: $\hat{\Psi} = \hat{A}_{0,1} \times \hat{A}_{1,2}$, where layers 0 and 2 are solid and layer 1 is fluid. Taking (3) into account, this matrix can be represented in the form

$$\hat{\Psi} = \begin{pmatrix} a & b^* \\ b & a^* \end{pmatrix}, \quad (5)$$

$$a = e^{-ik_1 l_1} \left[\cos(k_2 l_2) - i \frac{z_1^2 + z_2^2}{2z_1 z_2} \sin(k_2 l_2) \right],$$

$$b = -i \frac{z_2^2 - z_1^2}{2z_1 z_2} e^{-ik_1 l_1} \sin(k_2 l_2),$$

where $z_i = \rho_i c_i$ is the impedance of the corresponding layer ($i = 1, 2$); ρ_i is the density; c_i is the sound velocity; and $k_i = \omega/c_i$ and l_i are the wavenumber in the layer and its thickness, respectively.

In order to calculate the transfer matrix of a layered structure that consists of N pairs of layers, it is sufficient to raise the matrix $\hat{\Psi}$ to the N th power. To do this, let us use the formula [16]

$$\hat{\Psi}^N = \begin{pmatrix} a & b^* \\ b & a^* \end{pmatrix}^N = \begin{pmatrix} a \frac{\sin(N\varphi)}{\sin(\varphi)} - \frac{\sin((N-1)\varphi)}{\sin(\varphi)} & b^* \frac{\sin(N\varphi)}{\sin(\varphi)} \\ b \frac{\sin(N\varphi)}{\sin(\varphi)} & a^* \frac{\sin(N\varphi)}{\sin(\varphi)} - \frac{\sin((N-1)\varphi)}{\sin(\varphi)} \end{pmatrix},$$

where $\varphi = \arccos[\text{Re}(a)]$ is an auxiliary angle that is determined by the parameters of the layers.

With consideration for the above values of the elements of the transfer matrix of the layered structure, the transmission coefficient can be calculated from the formula

$$T = \frac{\sin(\varphi)}{a \sin(N\varphi) - \sin((N-1)\varphi)}.$$

Let us consider the transmission coefficient provided that the resonance frequencies of the fluid and solid layers differ exactly by a factor of 2: $k_1 l_1 = 2k_2 l_2 = \pi + 2\varepsilon$. In the approximation of a narrow transmission band ($\varepsilon \ll 1$), we have $a \approx \varepsilon(1 + 4\zeta) + 2i\zeta$. This yields

$$T \approx \frac{1}{\cos(N\varphi) + i\zeta \frac{\sin(N\varphi)}{\sin(\varphi)}}, \quad (6)$$

where $\varphi = \arccos[\varepsilon(1 + 2\zeta)]$, $\varepsilon = \frac{\pi}{2} \left(\frac{f}{f_1} - 1 \right)$, $\zeta =$

$\frac{z_1^2 + z_2^2}{2z_1 z_2}$, $f_1 = \frac{c_1}{2l_1}$ is the resonance frequency of the solid layer.

According to formula (6), the frequency dependence of the magnitude of the transmission coefficient consists of alternate peaks (maxima) and dips (minima). The latter do not reach zero but form a certain pedestal $|T|_{\min}$ (Fig. 4a, upper curve). In order to determine the height of this pedestal, let us consider the conditions for attaining the minimum in the transmission coefficient: $\cos(N\varphi) = 0$. From here, the pedestal is described by the formula

$$\begin{aligned} |T|_{\min} &\approx \frac{|\sin(\varphi)|}{\zeta} \approx \frac{\sqrt{1 - [\varepsilon(1 + 2\zeta)]^2}}{\zeta} \\ &= \frac{1}{\zeta} \sqrt{1 - \left(\frac{f - f_1}{\Delta f} \right)^2}, \end{aligned}$$

where $\Delta f = 2f_1/\pi(1 + 2\zeta)$ is the band halfwidth provided that the frequency range is $f \in [f_1 - \Delta f, f_1 + \Delta f]$. The maximum value of the pedestal is

$$\max(|T|_{\min}) \approx \frac{1}{\zeta}.$$

The obtained formulas allow the conclusion that an increase in the ratio of the impedances of neighboring layers leads to narrowing of the transmission peaks and a diminished pedestal. These features must be taken

Measured thicknesses and sound velocities in glass plates

Number	Thickness, mm	Sound velocity, m/s
1	1.662 ± 0.008	5781 ± 31
2	1.630 ± 0.007	5791 ± 13
3	1.628 ± 0.005	5790 ± 17
4	1.654 ± 0.007	5761 ± 77
5	1.632 ± 0.006	5785 ± 31
6	1.653 ± 0.006	5786 ± 20

into consideration when planning experiments: when the pedestal height is small, the transmission peaks are more pronounced and can be better observed. When the impedance contrast is high, a small width of the peaks indicates the necessity of choosing a sufficiently small frequency step in measurements of the transmission spectrum of a layered structure.

Let us find both the frequencies at which dips between neighboring transmission peaks are positioned and the number of these dips. For this purpose, the following condition is used: $N\varphi = \frac{\pi}{2} + \pi n$. Substituting this condition into formula (6), we obtain the expression for the frequencies that correspond to the minima of the transmission-spectrum magnitude:

$$f = f_1 + \Delta f \cos\left(\frac{1}{N}\left[\frac{\pi}{2} + \pi n\right]\right), \quad n = 0, 1 \dots N - 1.$$

Let us perform the same calculations to determine the positions of the transmission peaks and use the following conditions: $\cos(N\varphi) = 1$ and $\sin(\varphi) \neq 0$; i.e., $N\varphi = \pi n$ and $\varphi \neq \pi n$:

$$f = f_1 + \Delta f \cos(\pi n/N), \quad n = 1 \dots N - 1.$$

It follows from the condition $N\varphi = \pi n$ that the number of peaks must be $N + 1$, but because of the condition $\varphi \neq \pi n$, the two end peaks are not realized. Thus, the frequency dependence of the magnitude of the transmission spectrum within one band has $N - 1$ transmission peaks and $N - 2$ dips between them [5]. Note that the number of transmission peaks coincides with the number of fluid-filled cavities in the layered structure. The total width of the peaks and the depth of the dips between them are determined by the ratio of the impedances of the solid and fluid layers.

EXPERIMENTAL SETUP

Achievement of an acoustic analog of the BO effect requires special selection of the thicknesses of solid- and fluid layers. We proceed from the fact that only the thickness of fluid layers is controlled in the experiment. It is then required to create conditions under which the acoustic energy is stored mainly in the fluid layers, while the solid-state layers play a passive role. As is known, the energy is stored in a layer of thickness l near the resonance frequency multiple of $c/(2l)$, where c is the sound velocity in the layer. Hence, solid plates

do not resonate (are passive) within the frequency ranges far from the frequencies $f_n^{(\text{solid})} = n \times c_{\text{solid}}/(2l_{\text{solid}})$, $n = 1, 2, \dots$. The fluid layers efficiently store energy near frequencies of $f_m^{(\text{fluid})} = m \times c_{\text{fluid}}/(2l_{\text{fluid}})$, $m = 1, 2, \dots$. In order to ensure the energy localization condition only in the fluid layers, it is necessary to select a characteristic signal frequency close to one of the frequencies $f_m^{(\text{fluid})}$ and the farthest from $f_n^{(\text{solid})}$. These requirements are, in particular, satisfied if the resonance frequencies of the fluid layers are in the middle between the resonance frequencies of the solid-state layers. At low frequencies, this condition corresponds to frequencies of $f \approx f_1^{(\text{fluid})} = 0.5 \cdot f_1^{(\text{solid})}$, thus, the chosen widths of the fluid and solid layers must be equal to a half- and quarter-wavelength, respectively. For example, let there be glass layers with a thickness of $l_{\text{solid}} \approx 1.6$ mm with a sound velocity of $c_{\text{solid}} \approx 6000$ m/s (see below). The wave frequency must then be close to $c_{\text{solid}}/(4l_{\text{solid}}) \approx 1$ MHz, and the fluid-layer thickness $l_{\text{fluid}} = 2l_{\text{solid}}c_{\text{fluid}}/c_{\text{solid}} \approx 0.8$ mm. The above estimates were used to select the parameters of the experimental setup that is described below.

As was mentioned above, a layered structure of alternating solid and fluid layers was chosen as the studied medium (a similar structure was used in [11]). The layer structure was a construction of six parallel glass plates that were immersed in water. The plates were square-shaped with sides 4 cm in length. The plate thicknesses were measured with a micrometer (these data are listed in Table 1). The spread at different points of the plates was within 8 μm ; i.e., the relative variations in the thickness of each plate were within 0.5%. As is seen from this table, the thicknesses of all six plates were the same to within a high accuracy. The sound velocity in glass was measured at room temperature by the pulse-echo method using short signals, which were excited by the opticoacoustic method [17]. The results of these measurements are also shown in the table. The glass density was determined by weighing samples and measuring their dimensions; the density was 2503 ± 25 kg/m³. This value is in good agreement with the tabulated value for the window glass [18]. It was used in numerical calculations. The values of the density and sound velocity in water were taken as 1000 kg/m³ and 1500 m/s, respectively.

Note that the number of fluid layers in the above-described structure is smaller than the number of solid layers by unity; i.e., there were altogether five fluid layers with controlled thicknesses. As was pointed out above, the realization of an acoustic analog of the BO effect requires that the fluid-layer thicknesses l_m be set in accordance with formula (1). For this purpose, in our experiments, inserts with the required thickness were set between the glass plates. When the acoustic analog of BO was investigated, measurements were performed at different values of the gradient γ , thus

requiring a large number of inserts. Each insert consisted of a thick plate that roughly specified the layer thickness and a set of thin plates that ensured more accurate thickness adjustment. As the thick part of inserts, we used automobile clearance gages, which were plates of high-strength tool steel with calibrated thicknesses in the range from 50 μm to 1 mm. The thickness of the fluid layers was more finely adjusted by adding the required number of 10- μm -thick foil layers. The thus-formed inserts were strips with a length of 15 cm and a width of 1 cm. These strips were set at the opposite edges of glass plates. Thus, two inserts were used to specify the necessary distance between neighboring glass plates. The required value and high parallelism of the gap between the plates was checked with a micrometer by measuring the thickness of each insert near each of the four corners of the corresponding plate.

Figure 1 shows a schematic diagram of the experimental setup. The shape of a radiated signal in digital form was done by a computer (1) and transmitted to a digital generator (2). An analog signal from the generator arrived at a piezoelectric transducer (3), which, together with the studied structure (4), was in a water-filled pool (5). Acoustic waves excited by the transducer propagated in the water, passed through the layered structure, propagated again in the water, and arrived at the receiving transducer. The received signal then arrived at a digital oscilloscope (6), from which it was transmitted to the computer for recording and processing.

Two identical broadband transducers with a center frequency of ~ 1 MHz and a diameter of 38 mm (V392-

SU model, Olympus, United States) were used as the transmitting and receiving transducers. They were set opposite each other in optical adjustment devices, which allowed smooth control of the transducer tilt angles. Both adjustment devices were fixed to a rigid frame. One adjustment device was stationary, and the other could be moved along rails, thus making it possible to smoothly change the distance between the source and receiver.

In order to observe an acoustic analog of BO, the experimental setup must satisfy a number of requirements. In particular, (a) the layered structure must be plane-parallel, (b) the propagation of studied waves must be nearly one-dimensional, and (c) the source and receiver must have sufficiently broad frequency bands for undistorted transmission and reception of pulse signals.

The plane-parallelism of layers was guaranteed by the above-described process of the structure assembly. The one-dimensional character of propagating waves was ensured by the wide-aperture receiver and its position in the near-field zone. The length of the near-field zone can be evaluated as $L = \pi a^2/\lambda$, where $a = 1.9$ cm is the radius of the transducer aperture and $\lambda \approx 0.15$ cm is the wavelength at the center frequency. This estimate yields $L \approx 76$ cm, which appreciably exceeds the source-receiver distance used in the experiment (~ 30 cm). However, in reality, the near-field diffraction effects could be appreciable at shorter distances. In order to determine the degree of influence of wave divergence on the amplitude of acoustic waves, we preliminarily measured the received signals at different transmitter-receiver distances. These measurements

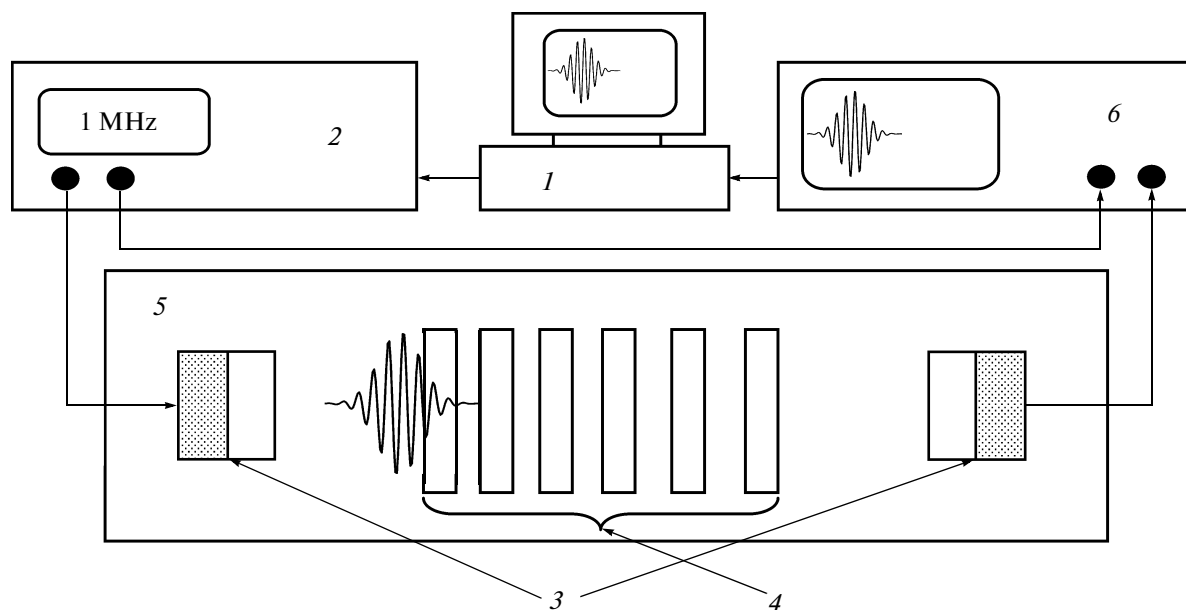


Fig. 1. Schematic of experimental setup: (1) computer, (2) generator, (3) piezoelectric transducers, (4) layered structure, (5) bath with water, and (6) oscilloscope.

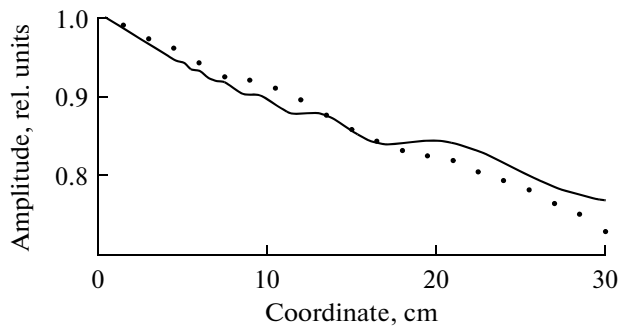


Fig. 2. Dependence of received acoustic signal on distance between transmitter and receiver: (solid line) experiment and (dotted line) theory.

were performed using an automated translational system that could displace the receiver with a step of $10\ \mu\text{m}$ along three mutually perpendicular axes (Velmex, United States). One of the axes that was perpendicular to the surfaces of the transducers was used to set the distance; two other axes, to bring the centers of the transmitter and receiver into coincidence. The transducers were adjusted before measurements. First, they were brought toward each other until contact to bring their centers into coincidence and to approximately set their surfaces in parallel positions. The receiver was then moved to the maximum possible distance (30 cm) under the experimental conditions, where the parallelism of the transducer was finely adjusted by setting the maximum amplitude of the received signal during transmission of a high-frequency signal. Subsequently, the distance between the transducers was again reduced almost to zero in order to test their coaxiality. If the coaxiality was violated, it was corrected by a transverse displacement of the receiver. The described adjustment procedure was repeated until the result became reproducible.

The effect of diffraction-limited divergence was studied by recording the amplitude of received acoustic waves as a function of the distance upon emission of a long radio pulse with a rectangular envelope and harmonic filling. Such measurements were performed at different frequencies. The use of a pulsed mode made it possible to avoid the influence of repeated reflections between the transmitter and receiver. Figure 2 shows the experimental dependence (dots) of the signal amplitude at a frequency of 800 kHz on the distance between the transducers. The solid line is the theoretical dependence for a piston transmitter that was obtained using the method described in [19]. For convenience of the comparison, both dependences were normalized to the corresponding maximum values. As is seen, the experimental dependence is properly described by the theoretical curve. In this case, the both curves indicate a certain decline in the wave amplitude with an increase in the distance to the receiver. Note that up to a distance of 30 cm, the signal did not decrease by more than 25%, thus allowing the

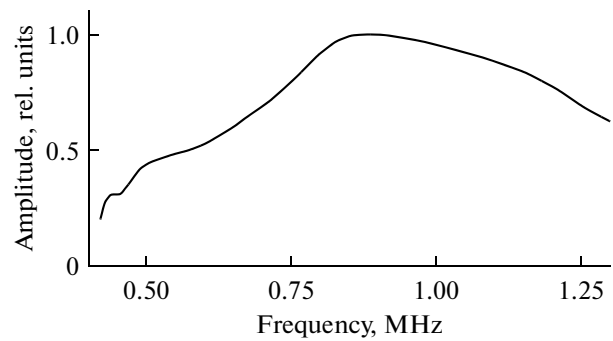


Fig. 3. Frequency response of transducers measured using a pulsed method at a distance of 20 cm between transducers.

diffraction-limited divergence to be considered weak in this region.

As was mentioned above, an analog of BO can be observed if the transmitter and receiver possess sufficiently wide frequency bands. This condition was checked via emission and reception of a short pulse for a 30-cm distance between the transducers (exactly this distance was used in the subsequent experiments with the layered structure). First, the parallelism of the transducers was adjusted using the above-described scheme. Then, a short electric radio pulse $u_1(t)$, whose spectrum $S_1(f)$ occupied a frequency band of $\sim 500\ \text{kHz} - 1.5\ \text{MHz}$, was fed to the transmitter. An excited acoustic pulse propagated in the water and arrived at the receiver, at whose output an electric signal $u_2(t)$ was recorded. In order to select the frequency response of the transducers, the received signal $u_2(t)$ was recorded from the moment of arrival of the signal front to the moment of arrival of a pulse that was reflected from the transmitter (i.e., the duration of the time window was equal to the time of the triple path from the transmitter to the receiver). The corresponding spectrum $S_2(f)$ was then calculated. In order to take the double electroacoustic transformation (during transmission and reception) into account, the efficiency of transmission and reception at a specified frequency $G(f)$ was characterized by the square root of the ratio of the spectral amplitudes of the received and excited signals: $G(f) = \sqrt{S_2(f)/S_1(f)}$. Figure 3 shows the plot of this function, which is normalized to its maximum value. As is seen, the function $G(f)$ insignificantly changes within a frequency range of 800 kHz–1 MHz, thus guaranteeing correct measurements of the shapes of nonstationary acoustic signals in this frequency range.

CALCULATION AND EXPERIMENTAL RESULTS

Let us first consider the characteristic features of the transmission spectrum of the investigated layered structure. As was mentioned above, the chosen thick-

nesses of the liquid layers were such that the thickness resonance of the liquid layers of interest was observed at frequencies far from the thickness resonances of the solid plates. On this basis, the liquid-layer and solid-layer thicknesses were chosen to be close to a half- and quarter-wavelength, respectively, in the operating frequency range, as in [11]. The frequency of the lowest thickness resonance in glass plates calculated using the parameters from the table was 1.76 MHz. The chosen thickness of the average liquid layer in calculations was $l_0 = 0.845$ mm; this value corresponds to the resonance frequency $f_0 = 888$ kHz at a sound velocity in water of 1500 m/s. The calculation results of the transmission coefficient in a wide frequency range are shown in Figs. 4a and 4b for a strictly periodic structure ($\gamma = 0$) and for the case of a nonzero gradient of the reciprocal thicknesses of the liquid layers ($\gamma = 3\%$). The behavior of the transmission coefficient (Fig. 4a) is typical of periodically nonuniform media: the transmission bands (permitted bands) alternate with forbidden bands. Transmission bands of finite widths are localized in the region of the thickness resonances. Thus, there is a frequency band with a width of ~ 100 kHz near a frequency of 0.9 MHz, which is positioned around the fundamental thickness resonance of the liquid layers. The structure of this band is shown in more detail in the plot–inset above the main graph. The corresponding segment in the main plot is marked with vertical dashed lines. It is seen that in comparison to a certain pedestal in the frequency dependence of the transmission coefficient, there are peaks whose number coincides with the number of fluid layers (this feature was already discussed above). The next transmission band (as the frequency increases) is localized near the frequency of the thickness resonance of the solid-state plates (~ 1.8 MHz) that coincides with the frequency of the second thickness resonance of the fluid layers. Therefore, this band is wider than the previous one and the number of peaks contained in it is equal to the total number of layers in the structure. With a further increase in frequency, there is one more permitted band near a frequency of 2.7 MHz. This band is related to the third resonance of the fluid layers. The observed regularity recurs at higher frequencies. As the fluid-layer thicknesses change in accordance with formula (1), the general character of the frequency dependence of the transmission coefficient remains unchanged (Fig. 4b). However, the fine structure of the permitted bands changes. This can be seen in the inset, which shows the behavior of the transmission coefficient near the main thickness resonance of the fluid layers. It is seen that side peaks in the fine structure begin to decrease. Another specific feature is more important: the pedestal decreases and the distance between the latter peaks begins to increase as compared to the case of $\gamma = 0$. Note that it is exactly these peaks in the permitted band that form the analog of the Wannier–Stark ladder. Their behavior with an increase in γ is discussed below in more detail.

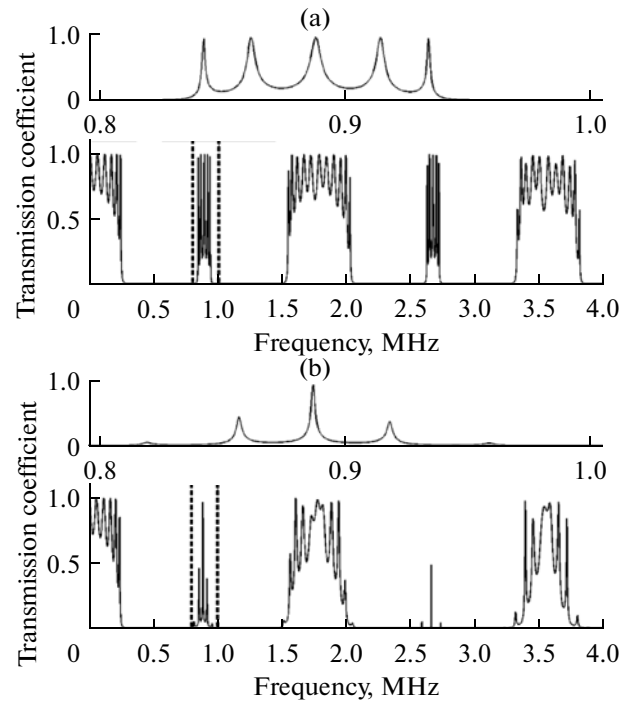


Fig. 4. Frequency dependence of transmission coefficient of layered structure for different reciprocal-thickness gradients: (a) $\gamma = 0\%$ and (b) $\gamma = 3\%$.

The effect of spatial localization of electrons in various regions of a crystal as a function of the energy acquired by electrons is one of the fundamental features of the behavior of electrons under conditions when BO is displayed. Analogous localization in wave analogs of BO must manifest itself in the form of a spatial redistribution of the energies of waves of different frequencies. The above-described theoretical algorithm allows studying the localization character in the case of the acoustic analog of BO. As an example, Fig. 5 shows the calculated distribution of the energy density of the acoustic field for frequencies of 0.8–1 MHz inside the experimentally studied layered structure. The latter frequency range corresponds to a permitted band near the frequency of the lowest thickness resonance of the liquid layers. Numbers denote glass plates, between which fluid layers are located. For convenience in visualizing weak signals, shades of gray are put in correspondence to the energy density logarithms. The coordinate and the frequency (in megahertz) are plotted along the abscissa (glass plates 1.65 mm thick are denoted by numbers) and ordinate axes, respectively. In calculations of the energy density at each frequency, the result was normalized to the energy density in the incident wave. As is seen in the presented pictures, the wave energy in the chosen frequency range is predominantly localized in the liquid layers. The striped structure within each layer corresponds to peaks in the above-considered frequency dependence of the transmission coefficient. For con-

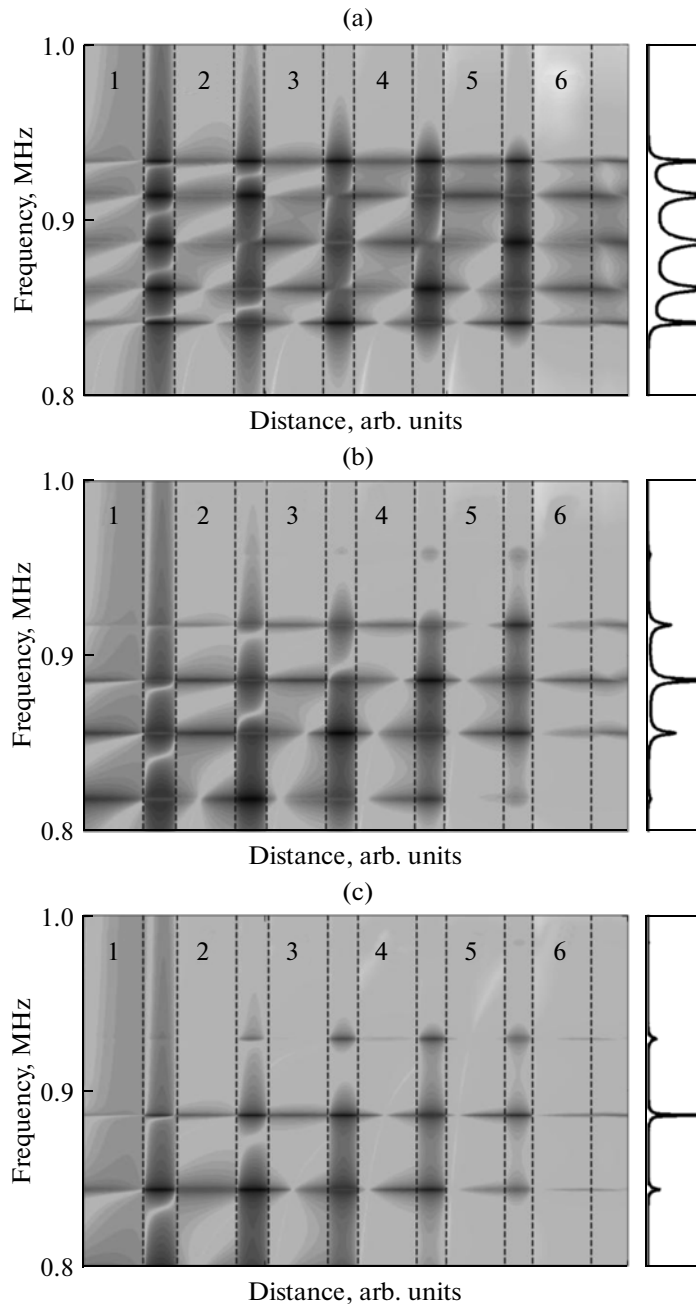


Fig. 5. Distribution of density of acoustic-field energy inside layered structure. Solid layers are marked with numbers. The frequency dependence of the transmission coefficient is shown in the inset (right). Data are presented for different reciprocal-thickness gradients: (a) $\gamma = 0\%$, (b) $\gamma = 3\%$, and (c) $\gamma = 5\%$.

venience, this dependence is shown in the inset to the right of the main image. Figure 5a corresponds to the case of identical thicknesses of the liquid layers ($\gamma = 0$). The wave energy at all frequencies is distributed approximately uniformly over the liquid layers; i.e., localization is absent. When a nonzero reciprocal-thickness gradient is introduced into the system, the character of the energy distribution changes (see Figs. 5b and 5c). The energy at low frequencies is localized on the left side, in thicker layers, while the

energy of the high-frequency components is stored on the right side of the structure, where the liquid layers are thinner. For large γ , the localization effect is more pronounced (Fig. 5c).

Another important feature of the changes that occur with an increase in g is a decrease in the density of the vibrational states (density of peaks on the frequency scale). As is seen in Fig. 5, this effect exactly corresponds to the behavior of the transmission peaks in the considered permitted band and is nothing but an

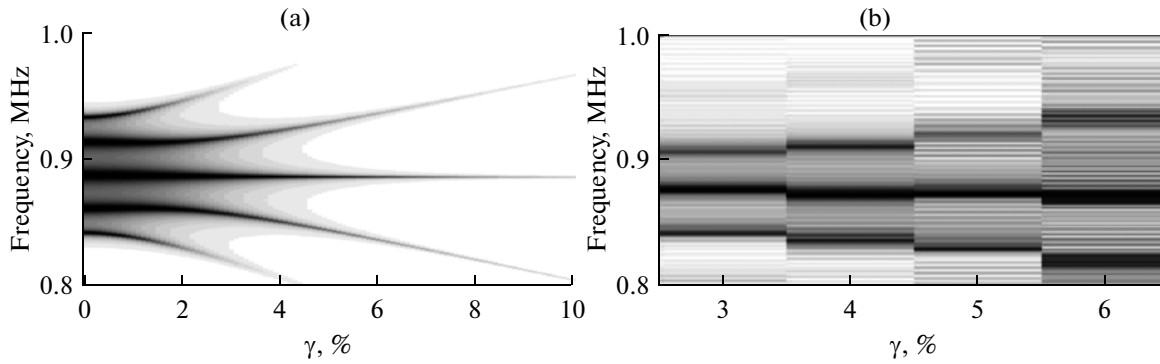


Fig. 6. Comparison of results of (a) simulating and (b) measuring the magnitude of the transmission coefficient (shade of gray) as functions of frequency (ordinate) and reciprocal-thickness gradient (abscissa).

analog of the effect of expansion of the Wannier–Stark ladder, which is observed with an increase in the external electric field in a crystal.

This phenomenon is shown in more detail in Fig. 6a, in which shades of gray show the calculated distribution of the transmission coefficient as a function of the frequency and the reciprocal-thickness gradient γ . An increase in γ from a zero value does not immediately cause an increase in the intervals between the transmission peaks. In the region of small γ , the intervals between the transmission lines remain virtually constant, but beginning already with $\gamma = 2\%$, they scatter almost linearly as a function of γ . In the same way, the difference in the frequencies of peaks in the electron spectrum is a linear function of the electric voltage applied to a crystal (the Wannier–Stark effect). An increase in γ also leads to a decrease in magnitude of the transmission coefficient at side peaks, which is associated with the substantial difference between the impedances of fluid and solid layers. It can be concluded from Fig. 6a that an acoustic analog of BO in the considered system can be observed in a range of γ of 2–8%.

The above-described theoretical results were compared to the experimental ones. The measurements were performed with the transducers set at a distance of 30 cm from each other. Before the studied multilayered structure was submerged in water, the parallelism of the receiver and transmitter surfaces was adjusted. For this purpose, a radio pulse with a rectangular envelope at a frequency of 1.1 MHz was emitted. The pulse duration was chosen as 40 periods: in this case, transient processes in the transducers terminated at the end of the pulse and the envelope reached a steady-state level that corresponded to continuous emission mode. The optimal positions of the transducers, in which the amplitude of the received signal in the region of the steady-state envelope was maximized, were sought by changing the tilt angles of the transducers. After this adjustment, the studied structure was placed between the transducers. The parallelism of the transmitter surface and the front-plate surface of the multilayer structure was also set using the acoustic

method according to the maximum amplitude of the plate-reflected signal.

The frequency dependence of the transmission coefficient of the layered structure was determined by comparing two runs of measurements—with and without the structure. The same amplitude (5 V) of the generator output pulse was used in both runs. The pulse duration was 40 wave periods. The amplitude of the received wave was measured in the time interval with a steady-state envelope of the receiver signal in approximately 15 periods after the arrival of the signal front, thus corresponding to the continuous-wave mode. The frequency was changed in a frequency band of 800 kHz–1 MHz with a step of 0.4 kHz. The transmission coefficient at each frequency was calculated as the ratio of the wave amplitudes in the presence and absence of the studied structure.

Figure 6b shows the results of experimental study of the frequency dependence of the layered-medium transmission coefficient for different γ . For proper comparison of the theoretical and experimental results, the data in Fig. 6b are represented in the same form as those in the theoretical curve in Fig. 6a. For this purpose, the curves of the frequency dependences at different γ are transformed into bands with a width $\Delta\gamma = 1\%$, the shades of gray in which characterize the transmission coefficient. Comparison of Figs. 6a and 6b shows that the experiment confirms the presence of a Wannier–Stark ladder with an almost linear divergence of the transmission peaks with an increase in the reciprocal-thickness gradient γ .

The frequency dependence of the transmission coefficient for $\gamma = 3\%$ is shown in more detail in Fig. 7. The theoretical and experimental dependences are shown by the upper and lower curves, respectively, and the coincidence is good. The only difference is a slight shift (~ 10 kHz) of the experimental “comb” with respect to the theoretical one toward lower frequencies. This shift amounts to approximately 1% of the frequency of the central model peak (890 kHz) and can be explained by the visible thickening of layers due to a certain nonparallelism of the transducer surfaces and layers in the layered structure.

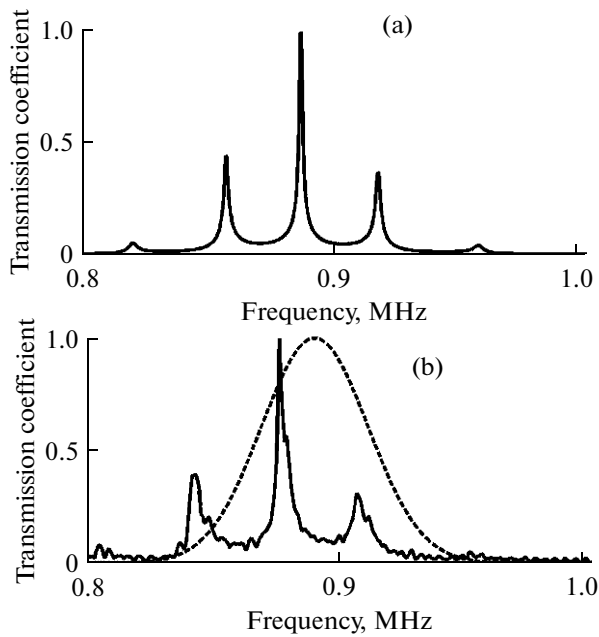


Fig. 7. Comparison of results of (a) simulating and (b) measuring the frequency dependence of the transmission coefficient for $\gamma = 3\%$. The dashed line shows the shape of the probing-pulse spectrum during observation of BO (Fig. 7b).

Observation of an analog of BO requires the appearance of a signal at the output of the layered structure, the spectrum of which must contain several (at least two) peaks of the Wannier–Stark ladder. As is seen in Fig. 7, this occurs if the spectrum of the incident wave falls within a transmission band, i.e., a frequency band that contains transmission peaks. The dashed line in the lower plot shows the bell-shaped spectrum of the incident wave chosen to implement BO. The center of the incident-wave spectrum was slightly displaced to the right relative to the most intense transmission peak in order to suppress this peak and amplify a weak peak—satellite, thus making the transmitted wave a composition of two quasi-monochromatic waves with comparable amplitudes.

Figure 8 shows the results of calculations (a) and measurements (b) of the BO effect observed upon incidence of a wave, whose spectrum is shown in Fig. 7b (dashed line), on the studied structure. The temporal profile of the incident signal is shown in the upper plots in Fig. 8. The signal has the shape of a radio pulse with a Gaussian envelope with a filling frequency of ~ 0.9 MHz and a duration of about $20 \mu\text{s}$. Other plots in Fig. 8 show the shape of a transmitted signal at different values of the reciprocal-thickness gradient γ . It is important that in the calculations and experiments, the transmitted signal had the form of pronounced quasi-periodic beats. The experimental

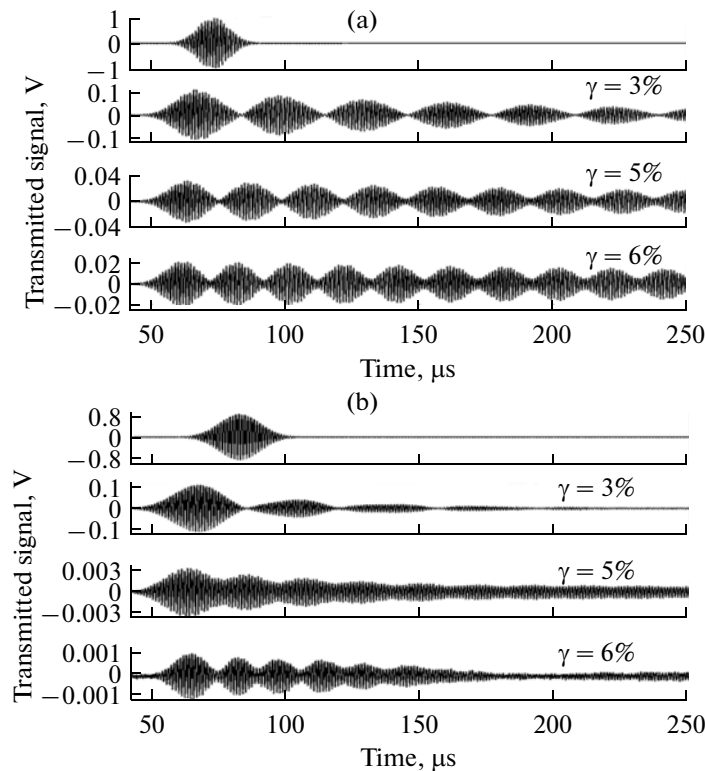


Fig. 8. Comparison of results of (a) simulation and (b) experiment of a signal measured at the output of the layered structure for $\gamma = 3, 5,$ and 6% . The upper plot shows the pulse signal incident on the structure.

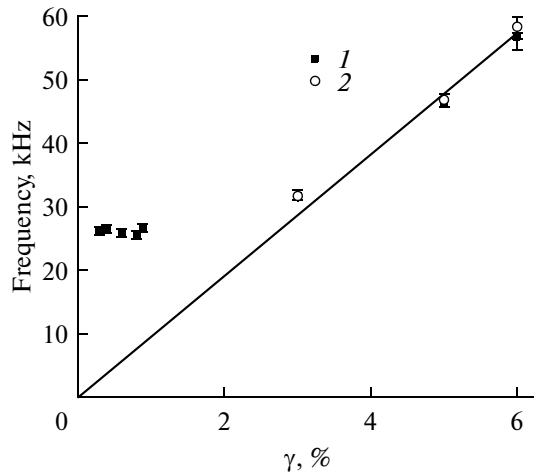


Fig. 9. Comparison of BO frequencies experimentally determined as the difference of the center frequencies of neighboring transmission lines (points 1) and directly measured from oscillations of the transmitted-signal envelope (circles 2). The solid line is the result of a linear approximation for measurements at $\gamma > 2\%$.

profiles of a signal from the receiving transducer decayed much more rapidly than the theoretical profiles; this can be explained by diffraction losses and structural imperfection. The lifetime of beats in the experiment was $\sim 150 \mu\text{s}$, thus allowing observation of several oscillations of the transmitted-signal envelope. As the reciprocal-thickness gradient γ increased, the oscillatory structure of the envelope remained constant and the oscillation frequency increased (see Fig. 8b). Thus, an acoustic analog of BO was observed.

Figure 9 shows the dependence of the BO frequency on the reciprocal-thickness gradient γ . The experimental points denoted by 1 were found from the spectral function of the layered-system transmission (curves of the type shown in Fig. 7b) on the basis of the frequency difference between the main transmission peak and peaks—satellites that close to it. The experimental points denoted by 2 were calculated proceeding from the envelope oscillation frequency (see Fig. 8b). In the region of $\gamma < 1\%$, the oscillation frequency was measured at a smaller step in the parameter γ in order to confirm the weak dependence of the beat frequency on the reciprocal-thickness gradient, predicted theoretically. This conclusion was confirmed experimentally. A range of $\gamma \geq 3\%$ is more interesting. In this region, the beat frequency increases almost linearly with an increase in the parameter γ . As is seen, the experimental points properly fall on a straight line drawn from the origin.

CONCLUSIONS

The use of the layered structure of plane—parallel plates the gaps between which are filled with a fluid makes it possible to achieve an effect analogous to the

quantum BO effect. In the acoustic case, the linear gradient of the reciprocal thicknesses of the fluid layers serves as an external electric field and the signal envelope undergoes oscillations at the output of the structure, on which a short pulse is incident. In this study, the first direct experimental observation of the acoustic analog of BO was performed using the structure of glass plates submerged in water. It was shown that an increase in the gradient of the reciprocal thicknesses of fluid layers leads to a linear increase in the oscillation frequency.

ACKNOWLEDGMENTS

This study was supported by the Russian Foundation for Basic Research, project nos. 08-02-00368 and 11-02-01189.

REFERENCES

1. F. Bloch, *Z. Phys.* **52**, 555 (1929).
2. C. Zener, *Proc. Roy. Soc. London* **145**, 523 (1934).
3. E. E. Mendez and G. Bastard, *Physics Today* **34** (1993).
4. G. H. Wannier, *Rev. Mod. Phys.* **34**, 645 (1962).
5. R. Tsu and L. Esaki, *J. Appl. Phys. Lett.* **22**, 562 (1973).
6. K. Leo, *Semicond. Sci. Technol.* **13**, 249 (1998).
7. T. Dekorsy, P. Leisching, K. Köhler, and H. Kurz, *Phys. Rev. B: Condens. Matter* **50**, 8106 (1994).
8. Yu. A. Kosevich, *Phys. Rev. B: Condens. Matter Mater. Phys.* **63**, 205313 (2001).
9. R. Sapienza, P. Costantino, and D. Wiersma, *Phys. Rev. Lett.* **91**, 263902 (2003).
10. L. Gutiérrez, A. Díaz-de-Anda, J. Flores, et al., *Phys. Rev. Lett.* **97**, 114301 (2006).
11. H. Sanchis-Alepuz, Yu. A. Kosevich, and J. Sanchez-Dehesa, *Phys. Rev. Lett.* **98**, 134301 (2007).
12. M. M. de Lima, Jr., Yu. A. Kosevich, P. V. Santos, and A. Cantarero, *Phys. Rev. Lett.* **104**, 165502 (2010).
13. N. D. Lanzillotti-Kimura, A. Fainstein, B. Perrin, et al., *Phys. Rev. Lett.* **104**, 197402 (2010).
14. L. M. Brekhovskikh and O. A. Godin, *Acoustics of Layered Media* (Springer, 1998).
15. A. E. Ponomarev, S. I. Bulatitskii, and O. A. Sapozhnikov, *Acoust. Phys.* **53**, 127 (2007).
16. Yariv, A. and Yeh, P., *Optical Waves in Crystals: Propagation and Control of Laser Radiation* (Wiley, New York, 1984).
17. A. A. Karabutov, L. I. Kobeleva, N. B. Podymova, and T. A. Chernyshova, *Zavod. Lab., Diagn. Mater.* **75** (3), 27 (2009).
18. Babichev, A.P., Babushkina, N.A., Bratkovskii, A.M., et al., in *Physical Quantities: Handbook*, Ed. by I.S. Grigor'ev and E. V. Melikhov (Energoatomizdat, Moscow, 1991).
19. R. Bass, *J. Acoust. Soc. Am.* **30**, 602 (1958).